Freeze-Out Parameters from Electric Charge and Baryon Number Fluctuations: Is There Consistency?

S. Borsanyi,[1] Z. Fodor,[1,2,3] S. D. Katz,[2,4] S. Krieg,[1,3] C. Ratti,[5] and K. K. Szabo[1,3]
[1]Department of Physics, Wuppertal University, Gauss Strasse 20, D-42119 Wuppertal, Germany
[2]Institute for Theoretical Physics, Eötvös University, Pázmány P. sétány 1/A, H-1117 Budapest, Hungary
[3]Jülich Supercomputing Centre, Forschungszentrum Jülich, D-52425 Jülich, Germany
[4]MTA-ELTE "Lendület" Lattice Gauge Theory Research Group, Pázmány P. sétány 1/A, H-1117 Budapest, Hungary
[5]Dipartimento di Fisica, Università di Torino and INFN, Sezione di Torino via Giuria 1, I-10125 Torino, Italy
(Received 2 April 2014; published 29 July 2014)

Recent results for moments of multiplicity distributions of net protons and net-electric charge from the STAR Collaboration are compared to lattice QCD results for higher order fluctuations of baryon number and electric charge by the Wuppertal-Budapest Collaboration, with the purpose of extracting the freeze-out temperature and chemical potential. All lattice simulations are performed for a system of $2+1$ dynamical quark flavors, at the physical mass for light and strange quarks; all results are continuum extrapolated. We show that it is possible to extract an upper value for the freeze-out temperature, as well as precise baryochemical potential values corresponding to the four highest collision energies of the experimental beam energy scan. Consistency between the freeze-out parameters obtained from baryon number and electric charge fluctuations is found. The freeze-out chemical potentials are now in agreement with the statistical hadronization model.

DOI: 10.1103/PhysRevLett.113.052301 PACS numbers: 25.75.-q, 12.38.Gc, 12.38.Mh, 24.60.-k

The fundamental theory of strong interactions predicts a transition from a hadronic system to a partonic one at sufficiently high temperatures or densities; this transition is an analytic crossover, as shown by lattice QCD simulations [1]. The conditions of temperature or density needed to create the deconfined phase of QCD can be reached in the laboratory: relativistic heavy ion collisions are contributing tremendously to our understanding of the QCD phase diagram and the properties of the quark-gluon plasma (QGP). The precision reached in the most recent lattice QCD simulations, as well as the increasing availability of data from the heavy ion experimental programs, allow us to compare the theoretical and experimental results in a very efficient way.

Fluctuations of conserved charges (electric charge, baryon number, and strangeness) are certainly a major example of this fruitful synergy. These observables, especially the higher order moments, were originally proposed as a signature for the QCD critical point [2–4], namely, the point of the phase diagram which marks the change from crossover to first-order phase transition. As a consequence, experimental results for moments of net-electric charge and net-proton multiplicity distributions have recently been published, in the collision-energy range $\sqrt{s}=7.7$–200 GeV covered by the RHIC beam energy scan [5–8]. The recent idea of extracting the freeze-out parameters of a heavy-ion collision through a comparison between lattice QCD results and experimental data has renewed the interest towards these observables even at $\mu=0$ [9–11].

In this Letter, we work under the assumption that in the evolution of a heavy-ion collision it is possible to identify two lines in the (T, μ_B) plane: a chemical freeze-out (at which all inelastic interactions cease) and a kinetic freeze-out (at lower temperature, at which elastic interactions cease). The particle multiplicities, and, therefore, the moments of their multiplicity distributions that we are using in our analysis, are fixed at the chemical freeze-out. As a first approximation, we assume that there are no inelastic processes beyond this point in the evolution of the system which can affect these observables. The chemical freeze-out has already been studied in terms of the statistical hadronization model by fitting a chemical potential and a temperature parameter to the pion, kaon, proton, and other accessible yields from experiment [12–15]. By decreasing the collision energy, the freeze-out chemical potential increases; repeating the analysis for a series of beam energies provides a freeze-out curve in the (T, μ) plane.

The comparison between the experimental and lattice QCD results for the electric charge and baryon number fluctuations allows a first-principles determination of the freeze-out temperature and chemical potential, under the assumption that the experimentally measured fluctuations can be described in terms of the equilibrium system simulated on the lattice. Possible experimental sources of nonthermal fluctuations are corrected for in the STAR data analysis: the centrality-bin-width correction method minimizes effects due to volume variation because of finite centrality bin width; the moments are corrected for the finite reconstruction efficiency based on binomial probability distribution [16]; the spallation protons are removed by appropriate cuts in p_T [8]. In general, effects due to

kinematic cuts are found to be small [17]. Besides, final-state interactions in the hadronic phase and nonequilibrium effects might become relevant and affect fluctuations [18,19]: a fundamental check in favor of the equilibrium scenario, in which multiplicity distributions of conserved charges are fixed at the chemical freeze-out, is the consistency between the freeze-out parameters yielded by different quantum numbers, e.g., electric charge and baryon number. In particular, while the freeze-out temperature might be flavor dependent [20], the chemical potentials as a function of the collision energy should be the same for all species. Therefore, in our approach we are able to check whether the three conserved charges B, Q, S have a common freeze-out surface, or whether the chemical freeze-out is a more involved scenario which allows different surfaces for different conserved charges. The present level of precision reached by lattice QCD results, obtained at physical quark masses and continuum extrapolated, allows us to perform this check for the first time.

One more caveat is in order, since experimentally only the net-proton multiplicity distribution is measured, as opposed to the lattice net-baryon number fluctuations. Recently it was shown that, once the effects of resonance feed-down and isospin randomization are taken into account [21,22], the net-proton and net-baryon number fluctuations are numerically very similar [23].

In this Letter we show for the first time that it is possible to find a consistency between the freeze-out parameters yielded by electric charge and baryon number fluctuations. This is achieved by systematically comparing our continuum-extrapolated results for higher order fluctuations of these conserved charges [11] to the corresponding experimental data by the STAR Collaboration at RHIC [7,8]. We are using the newly published, efficiency-corrected experimental results for the net-charge fluctuations and combine them with our lattice results presented in Ref. [11]. We also extract independent freeze-out conditions from the net-proton fluctuations and systematically compare the outcomes of the two. Details of the lattice simulations can be found in [11].

The fluctuations of baryon number, electric charge, and strangeness are defined as

$$\chi^{BSQ}_{lmn} = \frac{\partial^{l+m+n}(p/T^4)}{\partial(\mu_B/T)^l \partial(\mu_S/T)^m \partial(\mu_Q/T)^n}; \qquad (1)$$

they are related to the moments of the multiplicity distributions of the corresponding conserved charges. It is convenient to introduce the following, volume-independent ratios

$$\chi_3/\chi_2 = S\sigma; \qquad \chi_4/\chi_2 = \kappa\sigma^2,$$
$$\chi_1/\chi_2 = M/\sigma^2; \qquad \chi_3/\chi_1 = S\sigma^3/M. \qquad (2)$$

The chemical potentials μ_B, μ_Q, and μ_S are related in order to match the experimental situation: the finite baryon density in the system is due to light quarks only, since it is generated by the nucleon stopping in the collision region. The strangeness density $\langle n_S \rangle$ is then equal to zero for all collision energies, as a consequence of strangeness conservation. Besides, the electric charge and baryon-number densities are related, in order to match the isospin asymmetry of the colliding nuclei: $\langle n_Q \rangle = Z/A \langle n_B \rangle$. $Z/A = 0.4$ represents a good approximation for Pb-Pb and Au-Au collisions.

As a consequence, μ_Q and μ_S depend on μ_B so that these conditions are satisfied. This is achieved by Taylor expanding the densities in these three chemical potentials up to μ_B^3 [10]:

$$\mu_Q(T,\mu_B) = q_1(T)\mu_B + q_3(T)\mu_B^3 + \cdots,$$
$$\mu_S(T,\mu_B) = s_1(T)\mu_B + s_3(T)\mu_B^3 + \cdots. \qquad (3)$$

Our continuum extrapolated results for the functions $q_1(T), q_3(T), s_1(T)$, and $s_3(T)$ are shown in [11]. The quantities that we consider to extract the freeze-out T and μ_B, are the ratios $R^B_{31} = \chi^B_3/\chi^B_1$ and $R^B_{12} = \chi^B_1/\chi^B_2$, respectively, at values of (μ_B, μ_Q, μ_S, which satisfy the physical conditions discussed in the previous paragraph. As shown in Ref. [11], the leading order in χ^B_3/χ^B_1 is independent of μ_B, while the LO in χ^B_2/χ^B_1 is linear in μ_B. This allows us to use R^B_{31} to extract the freeze-out temperature; the ratio R^B_{12} is then used to extract μ_B (notice that our results for R^B_{12} are obtained up to NLO in μ_B).

We then independently extract μ_B from χ^Q_1/χ^Q_2 (which is also linear in μ_B to LO), in order to check whether different conserved charges yield consistent freeze-out parameters. In Ref. [11], we compared the lattice results for χ^Q_3/χ^Q_1 to the preliminary, efficiency-uncorrected data from the STAR Collaboration to extract an upper limit for the freeze-out temperature. We then obtained the corresponding chemical potentials by performing the same kind of comparison for χ^Q_1/χ^Q_2. The new, efficiency-corrected results for the moments of the net-charge multiplicity distribution from STAR show significant differences, compared to the uncorrected ones. This yields different values for μ_B, compared to the ones obtained in [11]. As for χ^Q_3/χ^Q_1, the experimental uncertainty on the corrected data is such that presently it is not possible to extract a meaningful freeze-out temperature from this observable.

In Fig. 1 we show the comparison between the lattice results for $\chi^B_3(T,\mu_B)/\chi^B_1(T,\mu_B)$ and the experimental measurement of $S_p\sigma^3_p/M_p$ by the STAR Collaboration [7]. The latter has been obtained for a 0%–10% centrality, at the four highest energies ($\sqrt{s} = 27$, 39, 62.4, and 200 GeV). Since the curvature of the phase diagram is small around $\mu_B = 0$ [24], this average allows us to determine the freeze-out temperature. The green-shaded area shows the valid temperature range: due to the uncertainty on the lattice results in the low-temperature

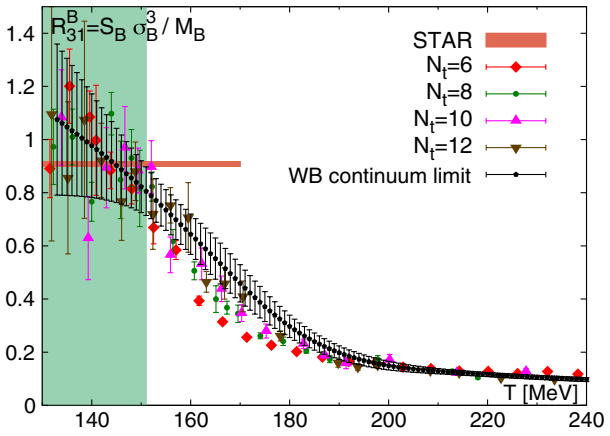

FIG. 1 (color online). R^B_{31}: The colored symbols show finite-N_t lattice QCD results. The continuum extrapolation is represented by black points (from Ref. [11]). The dark-orange band shows the recent experimental measurement by the STAR Collaboration [7]: it was obtained by averaging the 0%–5% and 5%–10% data at the four highest energies ($\sqrt{s} = 27$, 39, 62.4, and 200 GeV). The green-shaded area shows the valid temperature range.

regime, it is only possible to extract an upper value for the freeze-out temperature: the freeze-out takes place at a temperature $T_f \lesssim 151$ MeV, which is somewhat lower than expected from previous analyses [25] (allowing for a two-sigma deviation for the lattice simulations and the experimental measurements, the highest possible T_f is 155 MeV). In Refs. [26,27] we have published the lattice determination of the transition temperature from various chiral observables in the range 147–157 MeV. For the minimum of the speed of sound we found 145(5) MeV in [28]. The discussed freeze-out temperature is thus in the crossover region around or slightly below the central value.

We now proceed to determine the freeze-out chemical potential μ_B, by comparing the lattice results for R^B_{12} and R^Q_{12} [as functions of the chemical potential, and in the temperature range $(140 \le T_f \le 150)$ MeV] to the experimental results for M_p/σ^2_p and M_Q/σ^2_Q, published by the STAR Collaboration in Refs. [7,8,29]. This comparison is shown in the two panels of Fig. 2: the two quantities allow for an independent determination of μ_B from electric charge and baryon number: the corresponding values are listed in Table I, and shown in Fig. 3. Consistency between the two values of baryon-chemical potential is found for all collision energies (the nonmonotonicity of the lattice results for R^B_{12} at $\mu_B \ge 130$ MeV does not allow a determination of μ_B from this observable at $\sqrt{s} = 27$ GeV). Let us now compare the chemical potentials in Table I to those found earlier in statistical fits [12,14,30]. Plotting the parametrization of Refs. [12,30] together with our values we find a remarkable agreement (see Fig. 3). Note that, for the freeze-out temperature, statistical models typically yield a somewhat higher value: e.g., 164 MeV in Refs. [12,31]. Towards the lower end in the temperature range we find

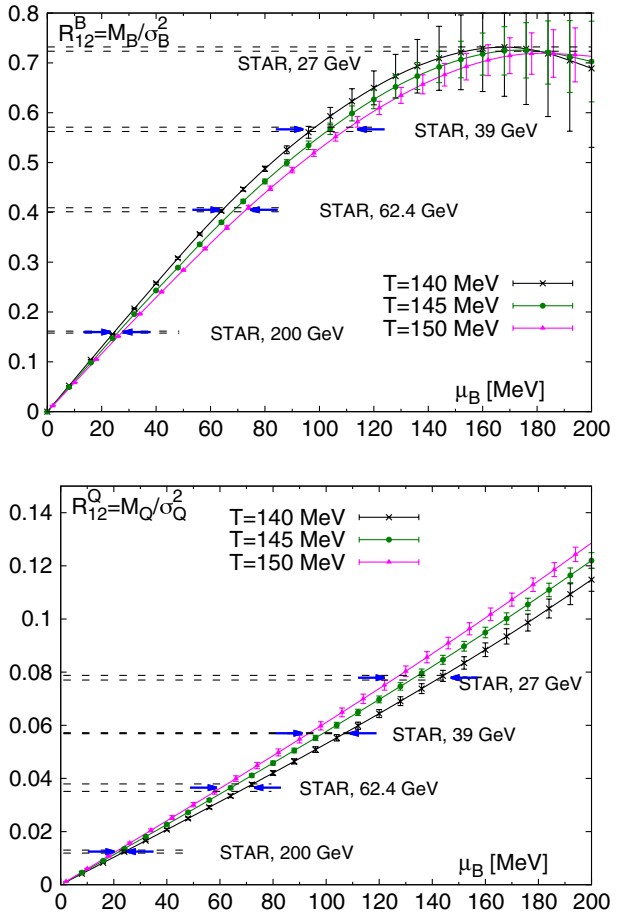

FIG. 2 (color online). Upper panel: R^B_{12} as a function of μ_B. The three points correspond to the STAR data for M_p/σ^2_p at collision energies $\sqrt{s} = 39$, 62.4, and 200 GeV and centrality 0%–10%, from Ref. [7] (the $\sqrt{s} = 27$ GeV point is also shown, but the nonmonotonicity of the lattice results at $\mu_B \ge 130$ MeV does not allow a determination of μ_B from it). Lower panel: R^Q_{12} as a function of μ_B. The four points correspond to the STAR data for M_Q/σ^2_Q at $\sqrt{s} = 27$, 39, 62.4, and 200 GeV and centrality 0%–10%, from Ref. [8]. In both panels, the colored symbols correspond to the lattice QCD results in the continuum limit, for the range $(140 \le T_f \le 150)$ MeV. The arrows show the extracted values for μ_B at freeze-out.

TABLE I. Freeze-out μ_B vs $\sqrt{s}$, for the four highest-energy STAR measurements. The μ_B values and error bars have been obtained under the assumption that 140 MeV $\le T_f \le$ 150 MeV. This uncertainty dominates the overall errors. Other (minor) sources of uncertainty are the lattice statistics and the experimental error.

$\sqrt{s}$ (GeV)	μ^f_B (MeV) (from B)	μ^f_B (MeV) (from Q)
200	25.8 ± 2.7	22.8 ± 2.6
62.4	69.7 ± 6.4	66.6 ± 7.9
39	105 ± 11	101 ± 10
27	⋯	136 ± 13.8

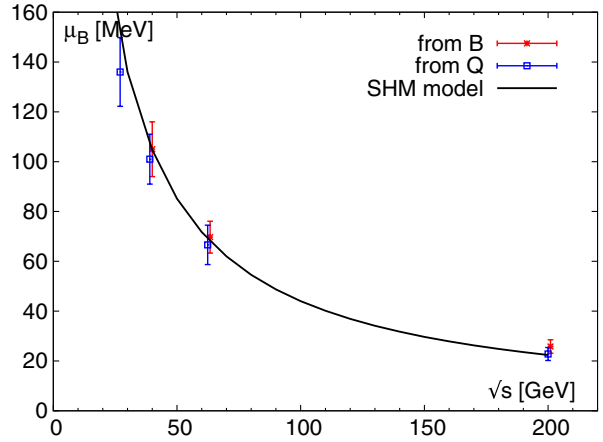

FIG. 3 (color online). Freeze-out chemical potential μ_B as a function of the collision energy. The red stars show the μ_B obtained by fitting R_{12}^B, the blue squares have been obtained by fitting R_{12}^Q. The black curve comes from the statistical hadronization model analysis of Refs. [12,30].

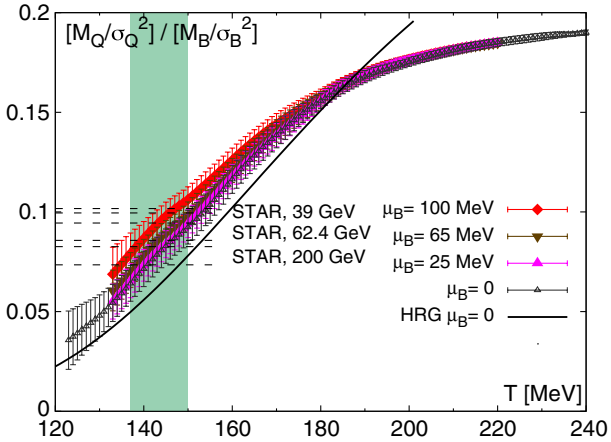

FIG. 4 (color online). R_{12}^Q/R_{12}^B: the colored symbols correspond to continuum-extrapolated lattice QCD simulations at different values of μ_B. The dashed lines show the recent experimental measurements by the STAR Collaboration [7,8] for a 0%–10% centrality and different collision energies. The green-shaded area shows the valid temperature range, $T_f = (144 \pm 6)$ MeV.

Ref. [32] with $T_f = 155 \pm 8$ MeV with $\mu_B = 25 \pm 1$ MeV, at $\sqrt{s} = 200$ GeV. The latest fit to particle ratios from the ALICE Collaboration [33] yields a temperature $T_f \simeq$ 156 MeV. However, this fit overestimates the protons, which would be optimally reproduced with a temperature consistent with the upper limit that we find in our analysis. The (multi-)strange particles clearly drive the particle ratio fit, and a final, decisive comparison between the freeze-out parameters obtained from the analyses of fluctuations from the lattice and of particle ratios from the SHM model can only be made if the measurement of the fluctuations of strangeness becomes available.

The comparison of our lattice results to the latest efficiency-corrected STAR data hints at a consistency of the freeze-out chemical potential if we assume an agreement in the temperature. This assumption was well motivated by the proton and charge skewness data. Let us now take the assumption further: if the freeze-out can be described by the same temperature and chemical potentials for charge and protons, then one can create a combined observable: $R_{12}^Q/R_{12}^B = [M_Q/\sigma_Q^2]/[M_B/\sigma_B^2]$. Here, the volume factor of the charge and baryon (proton) measurements cancel separately. Should our assumption be correct, this ratio of ratios is the preferable thermometer: it is far easier to obtain both for lattice and experiment since it does not involve skewness or kurtosis. We have lattice data available to $\sim\mu_B^2$ order, which we use when comparing our results to data. Such a comparison is shown in Fig. 4. Contrary to the skewness thermometer, here we see a clear monotonic temperature dependence without the hardly controllable lattice errors at low temperatures. The ratio R_{12}^Q/R_{12}^B is equal to $0.4\chi_2^B/\chi_2^Q$ at $\mu_B = 0$. Even if smaller in magnitude (due to the heavy nucleon mass vs the light pion mass), the rise of χ_2^B in the temperature range of interest is much faster than the one of χ_2^Q, as it is clear from Fig. 7 (right panel), in Ref. [34]. This allows for the identification of a narrow temperature band, instead of an upper limit.

The thermometer in Fig. 4 is, in fact, a consistency criterion: it agrees with the experimental data at the temperature which needs to be assumed for the freeze-out if the proton and charge fluctuations reflect the grand canonical ensemble at a common chemical potential. For high enough energies ($\sqrt{s} \geq 39$ GeV) this consistency is granted if freeze-out occurs in the range $T_f = 144 \pm$ 6 MeV. Notice that this temperature range lies just below the upper limit that we determined independently in Fig. 1.

In conclusion, in the present Letter we have extracted the freeze-out conditions (temperature and chemical potential) by comparing our continuum extrapolated lattice QCD results to the experimental moments of net-charge and net-proton multiplicity distribution by the STAR Collaboration. These new, efficiency corrected, experimental data point at a lower freeze-out temperature compared to previous estimates. This is compatible with the expectation that the freeze-out should occur just below the transition. The independent determinations of the freeze-out chemical potentials from electric charge and baryon number show a remarkable consistency with each other. This comparison is possible for the first time, and the consistency of the results is of fundamental importance to validate the hypothesis on which this method is based, namely, that the experimentally created system is close to thermal equilibrium at the freeze-out and can be described by lattice QCD simulations, at least in the light quark sector.

C. Ratti acknowledges fruitful discussions with Francesco Becattini, Rene Bellwied, and Bill Llope. This project was funded by the DFG Grant SFB/TR55. The

work of C. Ratti is supported by funds provided by the Italian Ministry of Education, Universities and Research under the Firb Research Grant RBFR0814TT. S. D. K. is funded by the ERC Grant [(FP7/2007-2013)/ERC No 208740] as well as the "Lendület" program of the Hungarian Academy of Sciences (LP2012-44/2012). The numerical simulations were performed on the QPACE machine, the GPU cluster at the Wuppertal University, and on JUQUEEN (the Blue Gene/Q system of the Forschungszentrum Juelich) and on MIRA at the Argonne Leadership Computing Facility through the Innovative and Novel Computational Impact on Theory and Experiment (INCITE) program of the U.S. Department of Energy (DOE).

[1] Y. Aoki, G. Endrodi, Z. Fodor, S. D. Katz, and K. K. Szabo, Nature (London) **443**, 675 (2006).
[2] M. A. Stephanov, K. Rajagopal, and E. V. Shuryak, Phys. Rev. D **60**, 114028 (1999).
[3] R. V. Gavai and S. Gupta, Phys. Rev. D **78**, 114503 (2008).
[4] M. Cheng *et al.*, Phys. Rev. D **77**, 014511 (2008).
[5] D. McDonald (STAR Collaboration), Nucl. Phys. **904–905**, 907c (2013).
[6] N. R. Sahoo (STAR Collaboration), Acta Phys. Pol. B Proc. Suppl. **6**, 437 (2013).
[7] L. Adamczyk *et al.* (STAR Collaboration), Phys. Rev. Lett. **112**, 032302 (2014).
[8] L. Adamczyk *et al.* (STAR Collaboration), arXiv: 1402.1558.
[9] F. Karsch, Central Eur. J. Phys. **10**, 1234 (2012).
[10] A. Bazavov *et al.*, Phys. Rev. Lett. **109**, 192302 (2012).
[11] S. Borsanyi, Z. Fodor, S. D. Katz, S. Krieg, C. Ratti, and K. K. Szabo, Phys. Rev. Lett. **111**, 062005 (2013).
[12] A. Andronic, P. Braun-Munzinger, and J. Stachel, Phys. Lett. B **673**, 142 (2009); **678**, 516 (2009).
[13] F. Becattini, J. Manninen, and M. Gazdzicki, Phys. Rev. C **73**, 044905 (2006).
[14] J. Cleymans, H. Oeschler, K. Redlich, and S. Wheaton, Phys. Rev. C **73**, 034905 (2006).
[15] J. Manninen and F. Becattini, Phys. Rev. C **78**, 054901 (2008).
[16] A. Bzdak and V. Koch, Phys. Rev. C **86**, 044904 (2012).
[17] P. Alba, W. Alberico, R. Bellwied, M. Bluhm, V. M. Sarti, M. Nahrgang, and C. Ratti, arXiv:1403.4903.
[18] J. Steinheimer, J. Aichelin, and M. Bleicher, Phys. Rev. Lett. **110**, 042501 (2013).
[19] F. Becattini, M. Bleicher, T. Kollegger, T. Schuster, J. Steinheimer, and R. Stock, Phys. Rev. Lett. **111**, 082302 (2013).
[20] R. Bellwied, S. Borsanyi, Z. Fodor, S. D. Katz, and C. Ratti, Phys. Rev. Lett. **111**, 202302 (2013).
[21] M. Kitazawa and M. Asakawa, Phys. Rev. C **85**, 021901 (2012).
[22] M. Kitazawa and M. Asakawa, Phys. Rev. C **86**, 024904 (2012); **86**, 069902 (2012).
[23] M. Nahrgang, M. Bluhm, P. Alba, R. Bellwied, and C. Ratti, arXiv:1402.1238.
[24] G. Endrodi, Z. Fodor, S. D. Katz, and K. K. Szabo, J. High Energy Phys. 04 (2011) 001.
[25] S. Mukherjee and M. Wagner, *Proc. Sci.*, CPOD2013 (2013) 039.
[26] Y. Aoki, S. Borsanyi, S. Durr, Z. Fodor, S. D. Katz, S. Krieg, and K. K. Szabo, J. High Energy Phys. 06 (2009) 088.
[27] S. Borsanyi, Z. Fodor, C. Hoelbling, S. D. Katz, S. Krieg, C. Ratti, and K. K. Szabó (Wuppertal-Budapest Collaboration), J. High Energy Phys. 09 (2010) 073.
[28] S. Borsanyi, G. Endrodi, Z. Fodor, A. Jakovac, S. D. Katz, S. Krieg, C. Ratti, and K. K. Szabo, J. High Energy Phys. 11 (2010) 077.
[29] The efficiency-corrected data for the lowest cumulant ratio (c_2/c_1) for net protons can be found on the public STAR website.
[30] A. Andronic, P. Braun-Munzinger, and J. Stachel, Nucl. Phys. **A772**, 167 (2006).
[31] J. Adams *et al.* (STAR Collaboration), Nucl. Phys. **A757**, 102 (2005).
[32] J. Rafelski, J. Letessier, and G. Torrieri, Phys. Rev. C **72**, 024905 (2005).
[33] M. Floris, Nucl. Phys. A (to be published).
[34] S. Borsanyi, Z. Fodor, S. D. Katz, S. Krieg, C. Ratti, and K. Szabo, J. High Energy Phys. 01 (2012) 138.